Effect of ion irradiation on the hardness properties of Zirconium alloy

HIWA MOHAMMAD QADR

Department of Physics, College of Science, University of Raparin, Sulaimanyah, Iraq

Email: hiwa.physics@uor.edu.krd

Abstract

An investigation into the irradiation of zirconium alloys with protons was carried out in this study. The effect of the irradiation induced hardening and also of the zirconium alloys was investigated by Vickers Hardness tests, in order to examine microstructural analyses. In addition, TRIM programme was used to identify the proton penetration depth. An irradiation at 3 MeV for a higher surface displacement rate was carried out with accompanying procedure for the calculation of dose in terms of displacements per atom using a binary collision approximation simulation program, a calculated dose of 0.0027- 0.0031 dpa depending on depth was found to increase the sample hardness by maximum mean of 10 *HV* between the irradiated and unirradiated zone of the sample, but variation over the surface of the sample as well as with depth makes this value statistically unreliable. Irradiations to higher dpa values for further investigation are supported by the conclusions of this work.

Keywords: Hardness, Zirconium, TRIM, ASTM.

Introduction

Although neutron irradiation always be necessary to test materials for reactor applications, ion beams can provide a lower cost and rapid mechanism for various purposes. An ion irradiation can be any charged particle beam, including electrons; protons or heavier nuclei [1-3]. One of the great advantages of ion irradiation is that it can be conducted for a specific energy, dose-rate and temperature, leading to a well-controlled experiment [4-6]. Furthermore, ion irradiation allows easy variation of these parameters over a wide range of values [7, 8]. Whereas, neutrons experiments, conducted in test reactors, can be very unspecific due to the variety of neutrons kinetic energies inside the reactor.

Additionally, the damage accumulation reached in ion irradiation is much higher than neutron ones. For instance, during a typical neutron irradiation experiment in a thermal test reactor, the end-of-life damage is 3-5dpa/year, likewise a fast reactor gives 20dpa/year. The average of end-of-life damage for components of a BWR core is 10 dpa, for PWR it is 80 dpa and for Advanced Fast Reactor it is 200 dpa [9]

Table 1 shows the chemical compositions of the Zicaloy-2 and Zirconium. Zirconium's applicability in nuclear reactors as fuel cladding comes from its very low thermal neutron capture cross-section (0.185 barn) [10-12], other metals such as steel are considered 'parasitic' to nuclear reactions because they capture a larger proportion of neutrons [13]. The purpose of the fuel cladding is then to provide a barrier to the coolant which is able to conduct heat while maintaining good mechanical properties and corrosion resistance. Zircaloy-2 is used in boiling water reactors [14], whilst reduced amounts of Ni allows Zircaloy-4 to be used in pressureised water reactors[15], Zr-Nb alloys are also used in CANDU, VVER and RBMK reactors [16] , zirconium low oxidation alloys are now also in use as PWR cladding [17]. Zircaloys are also used as structural components in grids, guide tubes and end plates of fuel assemblies [18-20].

Moreover, Vickers hardness test is important for both the micro scale and the macro scale, and has been investigated by many researcher [21-25]. The way the hardness value in a Vickers hardness test is deduced is as follows the two dimensions d_1 and d_2 and then inserted into below equation.

$$d = \sqrt{\frac{1.8544 * F}{HV}} \tag{1}$$

$$h = \frac{d}{7.0006} \tag{2}$$

Where *HV* is hardness value, *d* is intender diagonal, *F* is load and *h* is indentation depth. The Equation 1 was used in this work to find the indenter diagonal, the Equation 2 also is used to find the depth of indenter at using different loads. In this paper, the Stopping and Range of Ions in Matter (SRIM) was utilised to explore the irradiation effect on Zirconium alloy [26]. In addition, Microhardness for zirconium sample was measured using a Vickers hardness machine.

Table 1. Compositions of Zicaloy-2 and Zirconium (wt% or ppm) [27-29]

	Element								
	Sn	Fe	Cr	Ni	O	N	Hf	C	H
Zicaloy-2	1.1-1.5	0.07-0.2	0.1	0.05	0.12	0.008	0.02	0.027	0.0025
Zirconium		200 ppm	200 ppm		1000 ppm	100 ppm	2500 ppm	250 ppm	10 ppm

Materials and Methods

Once subjected to the irradiation programme, samples were micro hardness tested, as an investigation into the changes in mechanical properties inflicted by the proton beam. The procedure followed guidelines presented in the ASTM standard E384-11 [30].

The machine used was a Struers Durascan [31]. The micro hardness diamond indenter used was of the Vickers type, essentially a square based pyramid with diagonals 136º from the face. The samples used were 1 mm thick foils of zircaloy-2 – could not get zircaloy tubing. Prior to the irradiation programme, samples were polished to an average surface roughness of 1 μm.

The polishing procedure carried out was dependent on the material composition and the surface roughness as received. Precaution must be taken in this step to avoid improper polishing and grinding as cold working the surface of the sample could alter test results. It is important to note that not all of the samples were of the same geometry, but were all 100 μm thick. Irradiated samples were then mounted onto a flat surface using a sticky pad. Ensure the micro hardness tester is properly calibrated, and the diamond indenter fully raised from the testing plane. Care should be taken whilst placing the sample underneath the indenter, to avoid any contact with the diamond tip. Once the sample has been placed on the testing plane to a perpendicular position from the tester, it should not be moved until the hardness testing is completed. Using the tester software, a map of the indents should be created. In this case, the indents could be placed 0.5 mm apart.

The micro hardness testing machine was capable of producing and measuring indents formed by loads of 0.1, 0.3, and 1 kg. These loads can be specified for each indent placed on the indent map. Hardness values obtained from different loads however can not be compared discretely and any comparisons made between the two should be considering the trend of hardness change. Once an indent has been made, the diagonals can be measured from an optical photograph. For best results use higher magnifications. For the fully automated Struers machine, the indent formation, measurement and logging is done automatically along the indent map programmed by the operator. Approximately 100 indents can be recorded within an hour. The time for which the force is applied can be altered, in this case it was 10 s. This should agree with the ASTM guidelines of between 10 - 15 seconds [30].

Results

Calculation of displacement per atom (dpa) was done by using the SRIM software. The energies available to us in this experiment were 1, 3, 9 and 20 MeV. The comparative damage profiles of these for fixed beam parameters is shown in figure 1. Although the lower energies have taller Bragg peaks they do not distribute their energy through the material as much and so have much less dpa as an average through a sample. Thus, the plateau of the damage profile accessible from the surface increase with energy, when calculating dpa with depth of a sample the error from the TRIM damage profile reduces with increasing depth but the error from the gradient of the plateau for the average dpa increases.

Zircaloy-2 and pure zirconium were irradiated with 3 MeV protons for 20 minutes. Both samples were indented with 0.1 and 0.3 kg loads. The samples were predicted to have reached 0.003 dpa from SRIM software.

Hardness values were measured for irradiated and unirradiated zircaloy-2 using 0.1 and 0.3 kg loads. To measure hardness, one row of indentations was made separately for each load, and an average was taken. Vickers hardness test and error were then calculated.

For zircaloy-2 and pure zirconium, Vickers hardness values differ at the 0.1 and 0.3 kg loads. This difference occurred because of surface plastic and material elastic deformation, which are higher at lower load. These hardness decreased in proportion to an increase in indenter load.
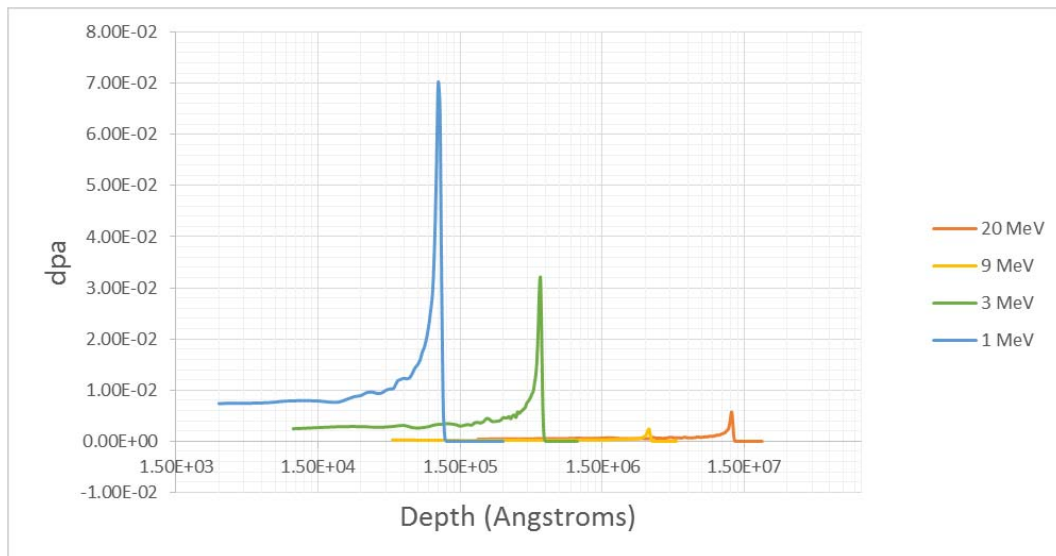
Figure 1: dpa value as a function of depth

Figures 2 and 3 show the hardness values across the surface of the sample. For the zircaloy-2, the irradiated zone was within the first 3 values either side of the x prole of the indents. The indents were made with varying loads; 0.1, 0.3 and 1 kg.

For the pure zirconium samples, indents were made with 0.1 and 0.3 kg loads, across the unirradiated zone for the first 5 measurements. The error bars used in Figures 2 and 3 were taken from the range of values in either zone.
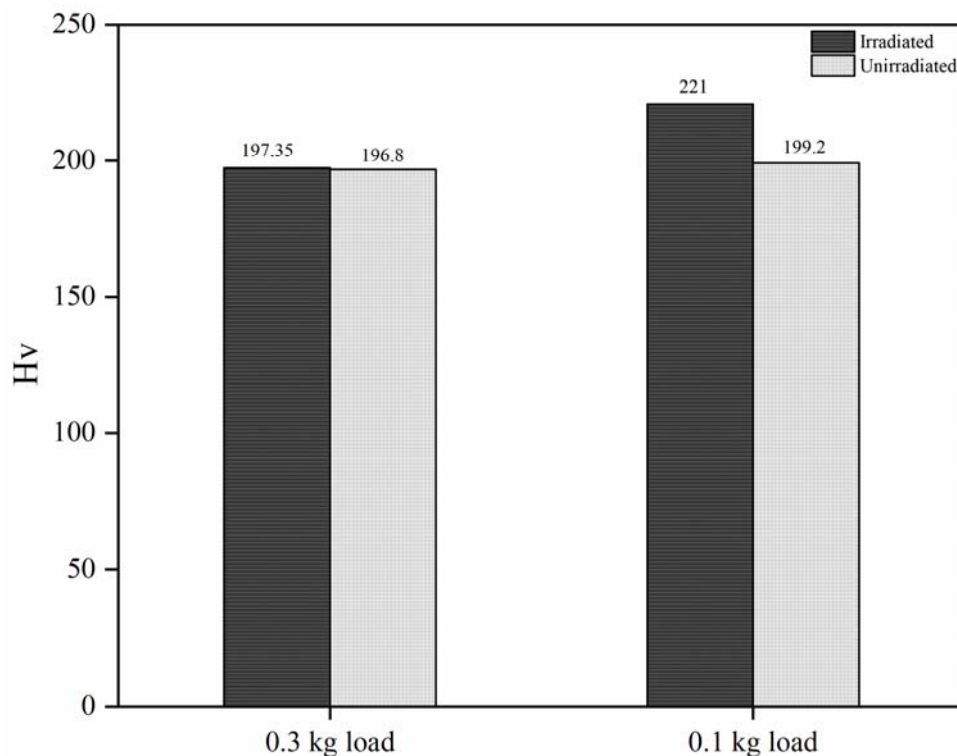

Figure 2: Vickers hardness value for irradiated and unirradiated pure zirconium using 0.3 and 0.1 kg loads
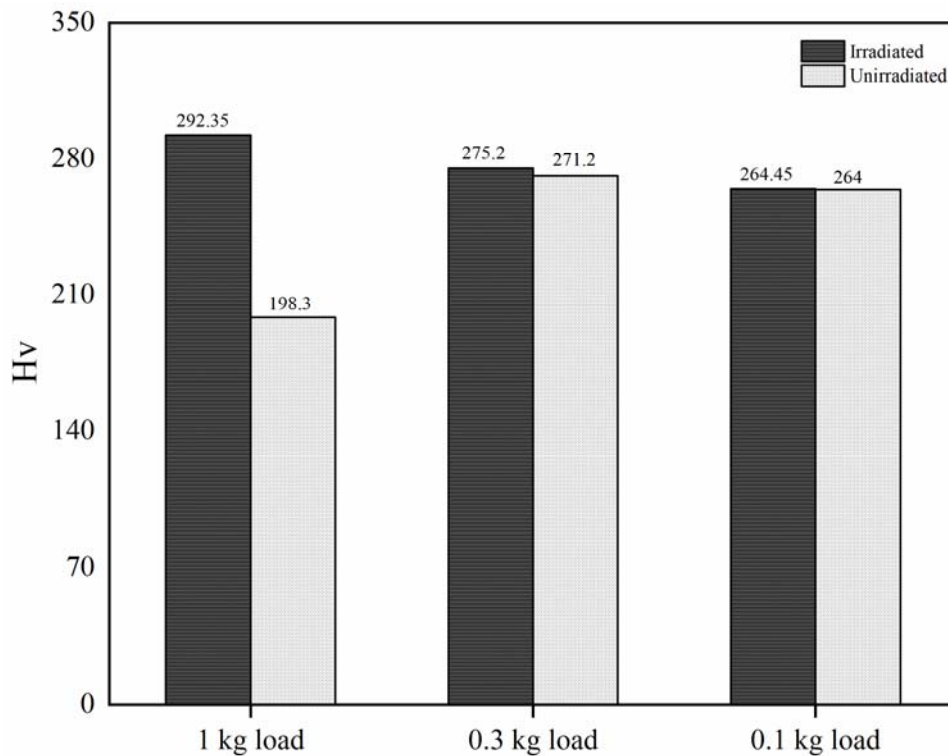
Figure 3: Vickers hardness value for irradiated and unirradiated zircaloy-2 using 1, 0.3 and 0.1 kg loads

Discussion

The precision of the hardness measurements made from the Vickers Hardness test vary with instrumentation and material factors, as well as measurement errors. The influential material factors to the testing include deformations to the indented shape caused by variance in the crystallographic and micro-structural texture. The offset of the diagonal lengths creates an error in the value measured. Also improper surface preparation can lead to errors in results obtained from low load testing, as residual deformation can influence the area indented. Ridging around the periphery of the indent can be caused from plastic deformation of the sample due to the load on the surface. This can cause inaccuracies in the measurement of the diagonals. It must also be noted that micro hardness testing etched surfaces will produce different hardness values to those obtained from testing an etched samples [30].

The main instrumental factors that influence hardness testing results centre around the angle between the indenter and the sample, and the nature of the force applied. The ASTM guideline specifies a maximum angle of 2° from the normal between the sample and the indenter. Any further deviation from the normal will produce non uniform indentations [30]. In addition, any vibrations present can cause differences in indentation depth. The influence of vibrations becomes larger as the load on the indenter decreases [32].

The accuracy of the Vickers hardness values calculated depends strongly on the diagonal measurements. The measurement of the diagonals of the indent into the sample surface can be done automatically and manually. In this case, the surface quality of the irradiated zone was

72

poor. This affected the ability of the hardness tester to measure the diagonals accurately, and consequently many of the measurements had to be altered manually. This action brings human bias into the error of the measurements. The nature of this error is quite random, as the operator could consistently over estimate, or consistently under estimate, or in fact could randomly both over and underestimate lengths of the diagonals.

The hardness value calculated is a function of the diagonal measurement, force and indenter geometry. To calculate the effect of variations in these parameters on the value calculated, differentials of the Vickers hardness calculations can be used:

$$dV = \frac{\partial V}{\partial P} dP + \frac{\partial V}{\partial d} dd + \frac{\partial V}{\partial \alpha} d\alpha \qquad (3)$$

In the above, α= 136º (angle of the vickers indenter), P is the load (measure in g) and d is the measured diagonal (in μm). Remembering the Vickers hardness relationship 1.

The precision of each variable was measured during the machines installation. They were reported as $dP = 0:005P$, $d\alpha = 6'$ and the precision of the diagonal measurement changed for different loads. At 100g load $dd = 1$μm, at 300g load $dd = 1$μm and at 1kg load $dd = 1.5$μm. The propagated errors for the machine turned out to be very small, approximately 0.005% of the hardness value. The reason for the greater variance in the measurements made at the lighter loads is unknown. It is proposed the texture of the microstructure on the surface of the sample effects the measurement at the lighter loads more. Further research into this area using XRD to perform texture measurements would be of interest.

Optical images shown in Figure 4 highlight possible sources of the variance in the hardness values obtained. According to the ASTM standard, the plastic deformation surrounding the indent (appearing as 'rippling') affects the accuracy to which the diagonals of the indent can be measured. Also the distortion of the indent shape can cause the hardness values to become invalid, as it indicates there is variation in the crystallographic and microscopic texture, as advised by the ASTM standard [30].

Shown by Figure 4-a and b, the surface of the sample in what was assumed to be the irradiated zones appears more dirty than the surfaces pictured in Figure 4-b and c.
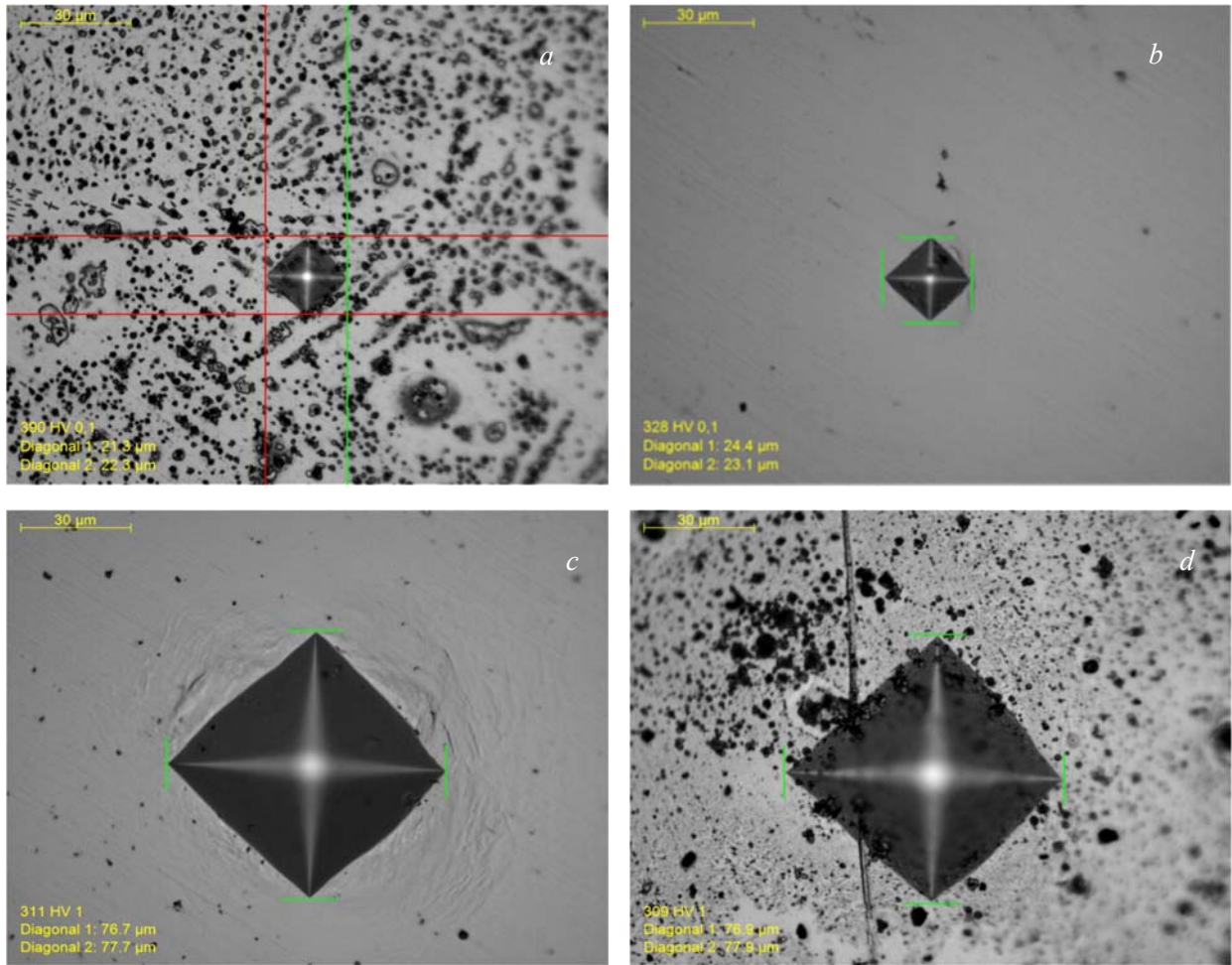
Figure 4. (*a*) dirty' surface of 'irradiated zone' (*b*) Irregular shape of indent at 0.1 kg load (*c*) Plastic deformation surrounding indent with 1 kg load and (*d*) Irregular shape of indent at 1 kg load

Conclusion

Due to the variance in results, it cannot be concluded that a change in hardness was displayed. To obtain reliable change in hardness, it would be recommended to test samples with larger amounts of dpa, with larger loads in order to avoid the variation in the mechanical properties at the surface do to the texture. In order to obtain more reliable evidence for a change in hardness at lower dpa's, it would be of interest to measure the hardness value prior to the irradiation, rather than compare the zone impinged with the proton beam to the zone protected by the aperture. It may be found that the hardening mechanisms may be more spread across the sample than anticipated.

References

[1] M. Durante, A. Golubev, W.-Y. Park, C. Trautmann, Physics Reports (2019).

[2] G. Was, Z. Jiao, E. Getto, K. Sun, A. Monterrosa, S. Maloy, O. Anderoglu, B. Sencer, M. Hackett, Scripta Materialia **88**, 33-36 (2014).

[3] H. M. Qadr, A. M. Hamad, Scientific Bulletin of Valahia University-Materials and Mechanics **17** (16), 18-27 (2019).

[4] P. Wady, A. Draude, S. Shubeita, A. Smith, N. Mason, S. Pimblott, E. Jimenez-Melero, Nuclear Instruments and Methods in Physics Research Section A: Accelerators, Spectrometers, Detectors and Associated Equipment **806**, 109-116 (2016).

[5] J. Gupta, J. Hure, B. Tanguy, L. Laffont, M.-C. Lafont, E. Andrieu, Journal of Nuclear Materials **501**, 45-58 (2018).

[6] C. D. Hardie, C. A. Williams, S. Xu, S. G. Roberts, Journal of Nuclear Materials **439** (1-3), 33-40 (2013).

[7] P. Singh, R. Kumar, in *Radiation Effects in Polymeric Materials* (Springer, 2019), pp. 35-68.

[8] H. Rath, B. Dash, A. Benyagoub, N. Mishra, Scientific reports **8** (2018).

[9] G. Was, R. S. Averback, in *Comprehensive Nuclear Materials* (Elsevier Ltd, 2012), pp. 195-221.

[10] Y.-I. Jung, H.-G. Kim, D.-W. Lee, Y.-S. Lim, S. Cho, Fusion Science and Technology **72** (3), 523-529 (2017).

[11] P. Ashcheulov, R. Skoda, J. Skarohlid, A. Taylor, F. Fendrych, I. Kratochvílová, Recent patents on nanotechnology **10** (1), 59-65 (2016).

[12] J. Nel, J. Havenga, M. Makhofane, A. Jansen, Journal of the Southern African Institute of Mining and Metallurgy **112** (1), 63-68 (2012).

[13] J. Feugeas, B. Gomez, G. Sanchez, J. Ferron, A. Craievich, Thin Solid Films **424** (1), 130-138 (2003).

[14] K. Geelhood, C. Beyer, presented at the Proceedings from the 2011 Water Reactor Fuel Performance Meeting, Chengdu, China, (2011).

[15] Z. Wang, H. Li, L. Xu, Q. Liu, L. Zha, S. Lin, INTERNATIONAL JOURNAL OF ELECTROCHEMICAL SCIENCE **13** (12), 12163-12171 (2018).

[16] A. Suri, Sadhana **38** (5), 859-895 (2013).

[17] M. Moorehead, Z. Yu, L. Borrel, J. Hu, Z. Cai, A. Couet, Corrosion Science **155**, 173-181 (2019).

[18] C. W. Solbrig, A. LaPorta, K. M. Wachs, J. R. Parry, Nuclear Material Performance, 57 (2016).

[19] M. Griffiths, P. Chow, C. E. Coleman, R. Holt, S. Sagat, V. Urbanic, "Evolution of microstructure in zirconium alloy core components of nuclear reactors during service", Effects of Radiation on Materials: Sixteenth International Symposium, (1994).

[20] R. M. Lobo, A. H. Andrade, M. Castagnet, (2011).

[21] W. Poole, M. Ashby, N. Fleck, Scripta Materialia **34** (4), 559-564 (1996).

[22] K. Herrmann, *Hardness testing: principles and applications*. (ASM International, 2011).

[23] R. P. Dewey, (Google Patents, 1945).

[24] E. Broitman, Tribology Letters **65** (1), 23 (2017).

[25] Y. Gao, H. Fan, Journal of materials science **37** (20), 4493-4498 (2002).

[26] J. F. Ziegler, M. D. Ziegler, J. P. Biersack, Nuclear Instruments and Methods in Physics Research Section B: Beam Interactions with Materials and Atoms **268** (11-12), 1818-1823 (2010).

[27] H. Takiishi, J. Duvaizen, I. Sato, J. L. Rossi, L. Pereira, L. G. Martinez, presented at the Materials Science Forum, 2012 (unpublished).

[28] A. Zieliński, A. Cymann, A. Gumiński, A. Hernik, G. Gajowiec, High Temperature Materials and Processes **38** (2019), 8-15 (2019).

[29] M. D. Gieselman, B. R. Dohner, K. Miyoshi, A. Sammut, P. E. Mosier, (Google Patents, 2019).

[30] I. ASTM, ASTM E384-10 (2010).

[31] W. M. Tucho, P. Cuvillier, A. Sjolyst-Kverneland, V. Hansen, Materials Science and Engineering: A **689**, 220-232 (2017).

[32] T. Sanponpute, A. Meesaplak, "Vibration effect on Vickers hardness measurement", IMEKO 2010 TC3, TC5 and TC22 Conferences Metrology in Modern Context, (2010).